Poly(*p*-phenylenevinylene) Derivatives Containing Electron-Transporting Aromatic Triazole or Oxadiazole Segments

Shinn-Horng Chen and Yun Chen*

Department of Chemical Engineering, National Cheng Kung University, Tainan, Taiwan, Republic of China

Received May 21, 2004; Revised Manuscript Received October 8, 2004

ABSTRACT: We report the synthesis, optical and electrochemical details, and properties of copolymers **P1**−**P3** consisting of alternate hole-transporting 1,4-bis(hexyloxy)-2,5-distyrylbenzene (HDB) and electron-transporting 4-(4-(hexyloxy)phenyl)-3,5-diphenyl- 4*H*-1,2,4-triazole (EDT) or 2,5-diphenyl-1,3,4-oxadiazole (EDO) segments linked via an ether spacer or a twisted σ-bond (biphenyl). These copolymers are soluble in common organic solvents such as chloroform, NMP, and 1,1,2,2-tetrachloroethane and exhibit good thermal stability with decomposition temperatures higher than 375 °C. **P1**−**P3** show efficient energy transfer from EDT or EDO to EDO fluorophores when photoexcited. Optical and electrochemical properties of **P1**−**P3** are also investigated in detail by comparing with **P4** and **P5** containing similar chromophores. From the cyclic voltammograms the onset oxidation and reduction potentials for isolated **P1** and conjugated **P2** are comparable, indicating that the effect of the twisted σ-bond in **P2** is similar to that of the ether spacer in **P1**. The optimized geometries of **P2** and **P3** show that the torsion angle between HDB and EDT or EDO are 83.6° or 89.6°, respectively, based on MNDO semiempirical calculations. The large torsion angle in **P2** and **P3** significantly limits delocalization of charges between hole- and electron-transporting segments. Accordingly, in **P2** and **P3** the oxidation and reduction starts at the hole- and the electron-transporting, respectively, like those in isolated **P1**. The HOMO and LUMO energy levels of **P1**, **P2**, and **P3**, estimated from electrochemical data, are −5.16, −5.12, and −5.19 eV and −3.35, −3.38, and −3.23 eV, respectively. Single-layer light-emitting diodes (Al/**P1**−**P3**/ITO) have been successfully fabricated, and they reveal blue or yellow electroluminescence.

Introduction

Electroluminescent (EL) polymeric materials are generally categorized into fully conjugated polymers, main-chain or side-chain polymers with isolated chromophores, and polymeric blends.[1−3] Among these materials π-conjugated polymers with donor−acceptor architectures are currently of interest because the electron or hole affinities can be enhanced[4] and the intramolecular charge transfer can lead to small band gap semiconducting copolymers for red emission.[5]

In our previous research[6−8] isolated copoly(aryl ether)s consisting of defined hole-transporting (donor) or electron-transporting (acceptor) segments did enhance electron and hole affinities simultaneously, among which the nonconjugated spacers conduced toward large band gap for blue emission. However, the characteristics, which normally occur in isolated polymers, are barely observed in conjugated polymers.

In the past the torsion effect on optical properties of conjugated polymers has been discussed frequently. The greater the torsion angle, the more diminished the effective conjugation length or reduced interchain interaction.[9−11] However, Bard et al. recently investigated electrogenerated chemiluminescence (ECL) and verified that the twisted structure between donor and acceptor groups in conjugated molecules leads to diminished electron delocalization and generation of localized radical cations and ions.[12,13] It seems that this specific characteristic in twisted structure can be incorporated into conjugated EL polymers with donor and acceptor groups.

* To whom correspondence should be addressed. E-mail: yunchen@mail.ncku.edu.tw.

In this work three copolymers **P1**−**P3** (Scheme 2), consisting of alternate isolated or covalently attached hole-transporting HDB and electron-transporting EDT[14−17] or EDO segments, have been synthesized and characterized. Furthermore, their optical and electrochemical properties are investigated by comparing with polymers **P4** and **P5** (as shown in Scheme 3) possessing similar structures.[18,19] The connection between hole- and electron-transporting segments of **P1**−**P5** can be divided into three types: (1) an ether spacer for **P1** and **P4**, (2) a single bond for **P2** and **P3**, and (3) a vinylene bond for **P5**. We studied the optical properties of **P1**−**P4** to elucidate the influence of conjugated and isolated structures. Furthermore, electrochemical properties of these polymers are also investigated in detail to evaluate the influence of geometric structures in **P2** and **P3**.

Experimental Section

Materials. The synthetic procedures of **16**, **17** (Scheme 2), **M2**, **M3**, **P4**, and **P5** (Scheme 3) have been described in the literature.[18,19] *N*-Methyl-2-pyrrolidone (NMP, Riedel-Dehaen Co.), *N*-cyclohexylpyrrolidone (CHP, Janssen Chimica Co.), chloroform ($CHCl_3$, Tedia Co.), tetrahydrofuran (THF, Tedia Co.), and other solvents were HPLC-grade reagents. All reagents were used without any further purification.

Instrumentation. All new compounds were identified by ^{1}H NMR, FT-IR, and mass or elemental analysis (EA). The ^{1}H NMR spectra were recorded on a Bruker AMX-400 MHz FT-NMR, and chemical shifts are reported in ppm using tetramethylsilane (TMS) as an internal standard. The FT-IR spectra were measured as a KBr disk on a Fourier transform infrared spectrometer, model Valor III from Jasco. Nominal and high-resolution mass spectra were recorded using an analytical mass spectrometer, model 70-250S, from VG. Elemental analysis was carried out on a Heraus CHN-Rapid elemental analyzer. Thermogravimetric analysis (TGA) of the

10.1021/ma048990m CCC: $30.25
Published on Web 12/13/2004

Scheme 1

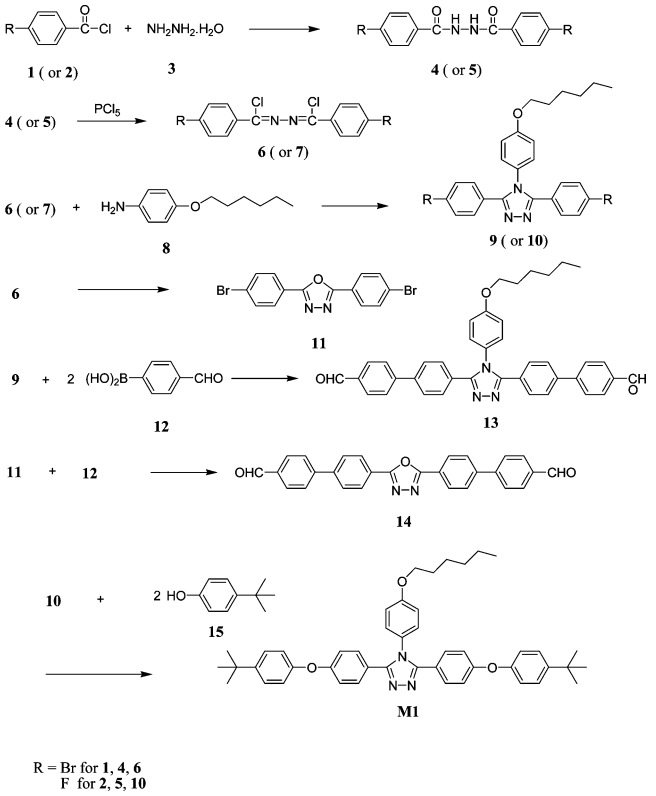

Scheme 2

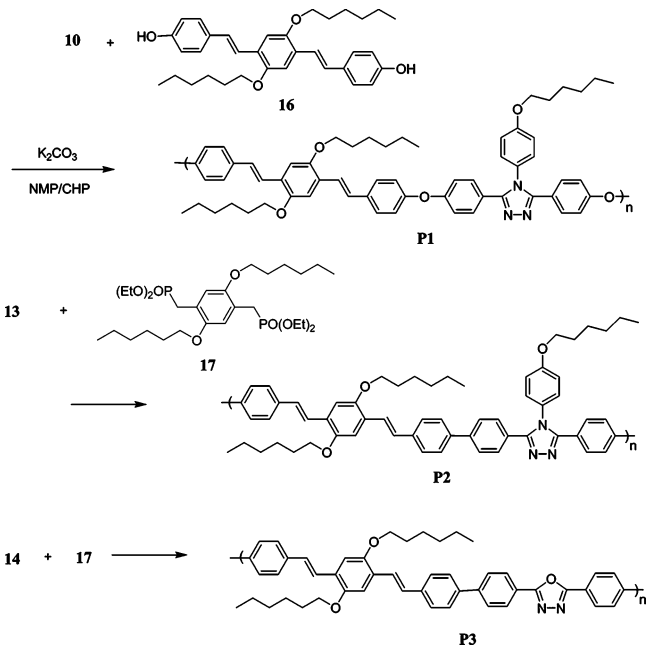

polymers was performed under nitrogen atmosphere at a heating rate of 20 °C/min using a Perkin-Elmer TGA-7 thermal analyzer. Thermal properties of the polymers were measured using a differential scanning calorimeter (DSC), Perkin-Elmer DSC 7, under nitrogen atmosphere at a 20 °C/min heating rate. UV−vis spectra were measured on a Jasco V-550 spectrophotometer, and the photoluminescence (PL) spectra were obtained using a Hitachi F-4500 fluorescence spectrophotometer. The diagrammatic curves of cyclic voltammetry were measured on a BAS CV-50W at room temperature under nitrogen atmosphere using ITO glass as the working electrode, a Ag/AgCl electrode as the reference electrode, and a platinum wire electrode as the auxiliary electrode supported in 0.1 M $(n\text{-Bu})_4NClO_4$ in acetonitrile. The energy levels were calculated

Scheme 3

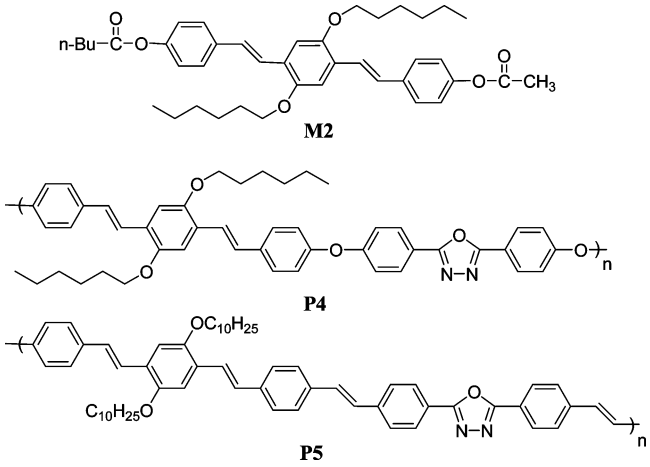

using the ferrocence (FOC) value of −4.8 eV with respect to vacuum level, which is defined as zero.[20] Single-layer light-emitting diodes with a configuration of Al/**P1**−**P3**/ITO were fabricated by spin coating polymer layer. The film thickness was about 60−100 nm as measured by atomic force microscopy (AFM). The thin aluminum layer was deposited as the cathode by thermal evaporation under a vacuum about 10^{-5} Torr. The optoelectronic characteristics of these devices were measured by a Keithley power supply (model 2400), and the EL spectra of the device were also measured by an Ocean Optics usb2000 fluorescence spectrophotometer. Fabrication and characterization of the devices were under ambient environment.

Synthesis of Monomers (Scheme 1). *Synthesis of Compounds **9**−**11***. To a two-necked flask were added with 4-bromobenzoyl chloride (**1**; 1.32 g, 6 mmol) hydrazine monohydrate (**3**; 0.15 g, 3 mmol), and 15 mL of NMP. The mixture was allowed to react at room temperature for 5 h. After reaction was completely promoted, it was precipitated from distilled water. The appearing products were collected by filtration, washed with ethyl acetate, and dried in a vacuum oven to provide **4** (77%).

The mixture **4** (0.84 g, 2.1 mmol) and phosphorus pentachloride (0.96 g, 4.62 mmol) was dissolved in 10 mL of toluene and stirred at 120 °C for 3 h in a nitrogen atmosphere. Toluene was stripped off under vacuum, and the residue was washed with distilled water. The appearing solids were collected by filtration, dried, and recrystallized from ethanol and dichloromethane to afford yellow solids of **6** (85%).

The mixture of **6** (0.86 g, 2 mmol), 4-hexoxylaniline (0.39 g, 2 mmol), and 15 mL of *N*,*N*-dimethylaniline was stirred at 135 °C in a nitrogen atmosphere for 12 h. After reaction was completely promoted, 30 mL of 2 N $HCl_{(aq)}$ was added and the mixture was stirred for another 0.5 h. The solids were filtered, dried, and then purified by column chromatography on silica gel using ethyl acetate/*n*-hexane as the eluent. Evaporation of the eluent afforded **9** (40%). The procedures for compounds **5** (68%), **7** (91%), and **10** (48%) were analogous to those for **4**, **6**, and **9**, respectively. The ring closure of **6** in the presence of $POCl_3$ at the reflux temperature was carried out to yield compound **11** (41%).

4: mp > 200 °C. ^{1}H NMR (DMSO-d_6, ppm): δ 10.62 (s, 2H, −NH−), 7.85 and 7.83 (d, 4H, Ar H), 7.75 and 7.73 (d, 4H, Ar H). FT-IR (film, cm^{-1}): 3191 (−CONH−), 3016, 2839, 2558, 1684, 1609, 1495, 1468, 1322, 1072 (C−Br), 1011, 931, 840. Anal. Calcd for $C_{14}H_{10}Br_2N_2O_2$: C, 42.24; H, 2.53; N, 7.04. Found: C, 42.28; H, 2.64; N, 7.03.

5: mp > 200 °C. ^{1}H NMR (DMSO-d_6, ppm): δ 10.53 (s, 2H, −NH−), 7.99−7.95 (m, 4H, Ar H), 7.37−7.33 (m, 4H, Ar H). FT-IR (film, cm^{-1}): 3209 (−CONH−), 3012, 2844, 2558, 1609, 1579, 1461, 1222, 1100 (C−F), 1012, 857. Anal. Calcd for $C_{14}H_{10}F_2N_2O_2$: C, 60.87; H, 3.65; N, 10.14. Found: C, 60.82; H, 3.79; N, 10.11.

6: mp = 144−145 °C. ^{1}H NMR (DMSO-d_6, ppm): δ 7.99 and 7.97 (d, 4H, Ar H), 7.82 and 7.79 (d, 4H, Ar H). FT-IR

(film, cm^{-1}): 3171, 3080, 2804, 2297, 1910, 1784, 1579 (−N=N−), 1483, 1393, 1222, 1066 (C−Br), 1011, 920, 825. Anal. Calcd for $C_{14}H_8Br_2Cl_2N_2$: C, 38.66; H, 1.85; N, 6.44. Found: C, 38.67; H, 1.93; N, 6.45.

7: mp = 133−134 °C. ^{1}H NMR (DMSO-d_6, ppm): δ 8.14−8.10 (m, 4H, Ar H), 7.46−7.40 (m, 4H, Ar H). FT-IR (film, cm^{-1}): 3109, 3071, 1903, 1605, 1575 (−N=N−), 1504, 1402, 1297, 1230, 1155, 1096 (C−F), 928, 839. Anal. Calcd for $C_{14}H_8F_2Cl_2N_2$: C, 53.70; H, 2.58; N, 8.95. Found: C, 53.72; H, 2.78; N, 8.931.

9: mp = 179−180 °C. ^{1}H NMR (acetone-*d*, ppm): δ 7.57 and 7.56 (d, 4H, Ar H), 7.54−7.31 (m, 6H, Ar H), 7.06 and 7.04 (d, 2H, Ar H), 4.07−4.02 (m, 2H $-CH_2-$), 1.81−1.74 (m, 2H, $-CH_2-$), 1.50−1.38 (m, 2H, $-CH_2-$), 1.37−1.33 (m, 2H, $-CH_2-$), 0.92−0.88 (m, 3H, $-CH_3$). FT-IR (film, cm^{-1}): 2930, 2864, 1599, 1513 (C=N), 1468, 1257 (−C−O−C−), 1066 (C−Br), 1007, 1840. Anal. Calcd for $C_{26}H_{25}Br_2N_3O$: C, 56.24; H, 4.54; N, 7.57. Found: C, 56.02; H, 4.61; N, 7.58.

10: mp = 173−174 °C. ^{1}H NMR (acetone-*d*, ppm): δ 7.53−7.48 (m, 4H, Ar H), 7.33−7.31 (m, 2H, Ar H), 7.17−7.02 (m, 6H, Ar H), 4.06−4.01 (m, 2H $-CH_2-$), 1.83−1.74 (m, 2H, $-CH_2-$), 1.53−1.33 (m, 6H, $-CH_2-$), 0.92−0.87 (m, 3H, $-CH_3$). FT-IR (film, cm^{-1}): 3063, 2940, 2874, 1609, 1511 (C=N), 1479, 1256 (−C−O−C−), 1222, 1100 (C−F), 1024, 843. Anal. Calcd for $C_{26}H_{25}F_2N_3O$: C, 72.04; H, 5.81; N, 9.69. Found: C, 72.03; H, 5.83; N, 9.59.

11: mp > 200 °C. ^{1}H NMR (DMSO-d_6, ppm): δ 8.08 and 8.05 (d, 4H, Ar H), 7.85 and 7.83 (d, 4H, Ar H). FT-IR (film, cm^{-1}): 3080, 2930, 2362, 1930, 1604, 1543, 1478, 1393, 1272 (C−O−C), 1077 (C−Br), 1006, 835. Anal. Calcd for $C_{14}H_8Br_2O$: C, 44.25; H, 2.12; N, 7.37. Found: C, 44.29; H, 2.14; N, 7.37.

*Synthesis of Compounds **13** and **14***. Compounds **13** and **14** were synthesized by Suzuki biaryl coupling reaction as follows. To a two-necked 10-mL glass reactor **9** (1.11 g, 2 mmol), 4-formylbenzeneboronic acid **12** (0.76 g, 4.4 mmol), $Pd(Ph_3)_4$ (0.36 g, 0.31 mmol), 20 mL of toluene, 20 mL of ethanol (99%), and 10 mL of 2 M Na_2CO_3(aq) were added under nitrogen atmosphere. The mixture was allowed to react at 80 °C for 12 h. After reaction was completely promoted, it was poured into distilled water and extracted with chloroform. The organic layer was dried with anhydrous magnesium sulfate and vacuum concentrated. The crude product was purified by washing with *n*-hexane and ethyl acetate and then dried in a vacuum to afford compound **13** (64%). The synthetic procedure of **14** was analogous to **13** with a yield of 40%.

13: mp > 200 °C. ^{1}H NMR (acetone-*d*, ppm): δ 10.04 (s, 2H, −CHO), 8.03 and 8.00 (d, 4H, Ar H), 7.93 and 7.91 (d, 4H, Ar H), 7.79 and 7.76 (d, 4H, Ar H), 7.65−7.62 (d, 4H, Ar H), 7.45 and 7.42 (d, 2H, Ar H), 7.12−7.09 (d, 2H, Ar H), 4.06 (s, 2H $-CH_2-$), 1.83−1.74 (m, 2H, $-CH_2-$), 1.43−1.32 (m, 6H, $-CH_2-$), 0.88 (s, 3H, $-CH_3$). FT-IR (film, cm^{-1}): 2933, 2853, 1701 (−CHO), 1609, 1511 (C=N), 1479, 1247 (−C−O−C−), 1003, 843. HR-MS (EI with DCI probe) *m/z* (M^+) calcd for $C_{40}H_{35}N_3O_3$: 605.2678; obsd 605.2676.

14: mp > 200 °C. ^{1}H NMR (DMSO-d_6, ppm): δ 10.08 (s, 2H, −CHO), 8.30 and 8.28 (d, 4H, Ar H), 8.07−8.04 (m, 12H, Ar H). FT-IR (film, cm^{-1}): 3075, 2830, 1694 (−CHO), 1604, 1483, 1378, 1237 (C−O−C), 1201, 1006, 835. HR-MS (EI with DCI probe) *m/z* (M+) calcd for $C_{28}H_{18}N_2O_3$: 430.1317; obsd 430.1316.

*Synthesis of Model Compound **M1** (Scheme 1)*. To a two-necked 25-mL glass reactor was charged with **10** (0.22 g, 0.5 mmol), **15** (0.18 g, 1.2 mmol), 5 mL of solvent mixture of NMP/CHP (v/v = 1/1), and an excess amount of K_2CO_3 (0.166 g, 1.20 mmol). The reaction mixture was then heated to 170 °C and reacted for 48 h. After the reaction was completely promoted, the reaction mixture was poured into distilled water. The mixture was extracted with chloroform, and the extract was washed with distilled water, dried with anhydrous magnesium sulfate, and then concentrated under reduced pressure. The crude products were purified by column chromatography using ethyl acetate/*n*-hexane (v/v = 1/3) as eluent. Evaporation of the eluent afford white solid of **M1** (35%).

Table 1. Polymerization Results and Characterization of P1∼P3

	M_n[a] (10^4)	M_w[a] (10^4)	PDI[a]	T_d[b] (°C)
P1	2.05	5.04	2.45	377
P2	0.40	0.51	1.25	408
P3	0.37	0.50	1.51	403

[a] M_n, M_w, and PDI of the polymers were determined by gel permeation chromatography using polystyrene standards in $CHCl_3$. [b] The 5% weight-loss temperatures.

M1: mp = 161−162 °C. ^{1}H NMR (acetone-*d*, ppm): δ 7.45−7.42 (m, 8H, Ar H), 7.32−7.29 (m, 2H, Ar H), 7.04 and 7.01 (d, 2H, Ar H), 6.98 and 6.97 (d, 4H, Ar H), 6.89 and 6.87 (d, 4H, Ar H), 4.04−3.99 (m, 2H $-CH_2-$), 1.79−1.74 (m, 2H, $-CH_2-$), 1.51−1.43 (m, 2H, $-CH_2-$), 1.35−1.30 (m, 4H, $-CH_2-$), 1.27−1.24 (m, 18H, $-CH_3$), 0.92−0.87 (m, 3H, $-CH_3$). FT-IR (film, cm^{-1}): 2958, 2869, 1600, 1508 (C=N), 1474, 1247 (−C−O−C−), 1171, 1108, 1012, 831. Anal. Calcd for $C_{46}H_{51}N_3O_3$: C, 79.62; H, 7.41; N, 6.06. Found: C, 79.53; H, 7.47; N, 6.05.

*Synthesis of Polymers **P1**−**P3** (Scheme 2).* **P1**−**P3** were prepared by the nucleophilic displacement reaction or Horner−Wadsworth−Emmons reaction described as follows. To a two-necked 25-mL glass reactor **10** (0.22 g, 0.50 mmol), **16** (0.26 g, 0.50 mmol), 10 mL of toluene, 5 mL of solvent mixture of NMP/CHP (v/v = 1/1), and an excess of K_2CO_3 (0.166 g, 1.20 mmol) were added. The reaction mixture was then heated to 170 °C and reacted for 80 h. The toluene was removed by condensing in the Dean−Stark trap. The mixture was dropped into 150 mL of a methanol/distilled water (v/v = 2/1) mixture. The **P1** precipitates were collected by filtration and further purified by Soxhlet extraction for 24 h using isopropyl alcohol as solvent (yield 51%).

A two-necked flask 25-mL glass reactor was charged with **13** (0.31 g, 0.5 mmol), **17** (0.28 g, 0.5 mmol), 6 mL of NMP, and solid potassium *tert*-butoxide. The mixture was stirred at ambient temperature for 24 h and then precipitated in a large amount of methanol to isolate solid products. The **P2** was purified by Soxhlet extraction for 24 h using acetone as solvent (yield 61%). The synthesis procedure of **P3** was analogous to **P2** with a yield of 66%.

P1: ^{1}H NMR ($CDCl_3$, ppm) δ 7.49−7.43 (m, 12H, Ar H), 7.10−6.92 (m, 14H, Ar H), 4.05−3.97 (m, 6H $-CH_2-$), 1.87−1.46 (m, 6H, $-CH_2-$), 1.35−1.19 (m, 18H, $-CH_2-$), 0.97 (s, 9H, $-CH_3$). FT-IR (film, cm^{-1}): 2936, 2855, 1707, 1595 (C=N), 1506, 1471, 1241 (−C−O−C−), 1167, 1008, 841. Anal. Calcd for $C_{60}H_{65}N_3O_5$: C, 79.26; H, 7.32; N, 4.62. Found: C, 76.60; H, 6.57; N, 4.76.

P2: ^{1}H NMR ($CDCl_3$, ppm) δ 7.60−7.26 (m, 16H, Ar H), 7.03−6.82 (m, 8H, Ar H), 4.24−4.02 (m, 6H $-CH_2-$), 1.64−1.22 (m, 24H, $-CH_2-$), 0.94−0.92 (m, 6H, $-CH_3$). FT-IR (film, cm^{-1}): 2947, 2865, 1689, 1603 (C=N), 1509, 1471, 1245 (−C−O−C−), 1203, 962, 845. Anal. Calcd for $C_{60}H_{65}N_3O_3$: C, 82.25; H, 7.48; N, 4.80. Found: C, 80.78; H, 7.36; N, 4.94.

P3: ^{1}H NMR ($CDCl_3$, ppm) δ 8.26−8.23 (m, 4H, Ar H), 7.81−7.55 (m, 12H, Ar H), 6.93−6.82 (m, 4H, Ar H), 4.12−4.08 (m, 4H $-CH_2-$), 1.89−1.43 (m, 16H, $-CH_2-$), 0.95−0.75 (m, 6H, $-CH_3$). FT-IR (film, cm^{-1}): 2927, 2857, 1703, 1607 (C=N), 1486, 1420, 1203 (−C−O−C−), 1003, 962, 810. Anal. Calcd for $C_{48}H_{48}N_2O_3$: C, 82.55; H, 6.90; N, 4.00. Found: C, 79.60; H, 6.67; N, 3.93.

Results and Discussion

Synthesis and Characterization of Copolymers. The number-average (M_n) and the weight-average molecular weights (M_w) of **P1**−**P3**, determined by gel permeation chromatography using polystyrene as standard, are listed in Table 1. All the synthesized polymers were soluble in common organic solvents such as chloroform, NMP, and 1,1,2,2-tetrachloroethane. Thermal properties of the synthesized polymers were evaluated by TGA under nitrogen atmosphere. The weight losses were less than 5% on heating to 375 °C for each

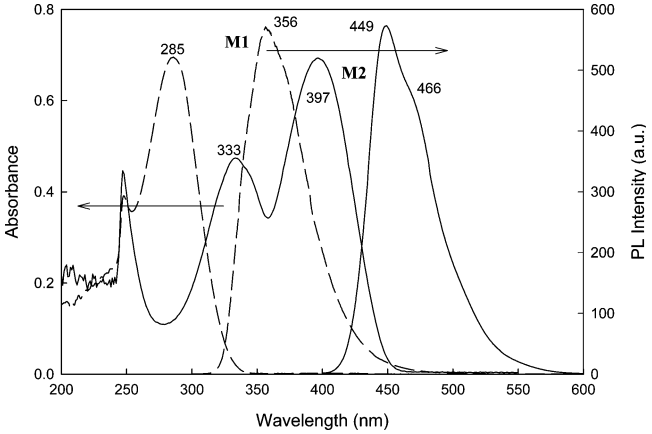

Figure 1. Photoluminescence (excitation = 285 nm for **M1** and 397 nm for **M2**) and UV−vis absorption spectra of model compound **M1** (- -) and **M2** (—) in $CHCl_3$ solutions of 1×10^{-5} M.

polymer. No melting temperature and obvious glass-transition temperature were observed below 300 °C in the DSC thermogram. The polymerization and characterization results of **P1**−**P3** are tabulated in Table 1.

Optical Properties. Figure 1 illustrates the absorption and photoluminescence spectra (in $CHCl_3$) of model compounds **M1** and **M2**, which, respectively, simulate the isolated EDT and HDB fluorophores of **P1**. The emission peaks of **M1** and **M2** are located at 356 and 449 nm, respectively. For isolated copolymers **P1** it is reasonable that its emissions originate from the isolated fluorophores, i.e., electron-transporting EDT and hole-transporting segment HDB segments. As shown in Figure 2, however, the PL spectra of **P1** (excitation at 388 nm) are mainly dominated by HDB fluorophores with longer emissive wavelength and show a maximum peak at 453 nm. This indicates that efficient excitation energy transfer from EDT fluorophores to HDB fluorophores has occurred in **P1**. The emission spectra of **M1** overlap greatly with the absorption of **M2** (Figure 1), suggesting that excitation energy might transfer from **M1** (energy donor) to **M2** (energy acceptor) if the distance between **M1** and **M2** is close enough. To ascertain this presumption, PL spectral transforms of **M1** and **M2** mixture in $CHCl_3$ upon increasing concentration are traced. As shown in Figure 3 the relative intensity of **M2** ($\lambda_{max} = 450$ nm), as compared to that of **M1** ($\lambda_{max} = 356$ nm), significantly enhances when the concentration was increased from 5×10^{-6} to 5×10^{-5} M. The transformation of the PL spectra (excitation at 285 nm) with concentration would be caused by increased reabsorption and excitation energy transfer due to reduced intermolecular distance, which is mainly controlled by concentration in solution. Accordingly, **P1** shows only one peak at 453 nm that must be due to efficient intrachain energy transfer because EDT (energy donor) and HDB (energy acceptor) segments are connected only via an ether spacer. Similar efficient energy transfer has also been observed in polymers **P2**−**P4** (Figure 2). The relative phenomenon has been discussed in our previous work.[19]

The PL spectra of **P1**, **P2**, **P3**, and **P4** in $CHCl_3$ solution exhibit peaks at 453, 476, 487, and 452 nm, respectively, as shown in Figure 2. The PL spectral peaks of isolated **P1** and **P4** reveal a blue shift of 23 and 35 nm, respectively, as compared with those of conjugated **P2** and **P3**. This is due to diminished

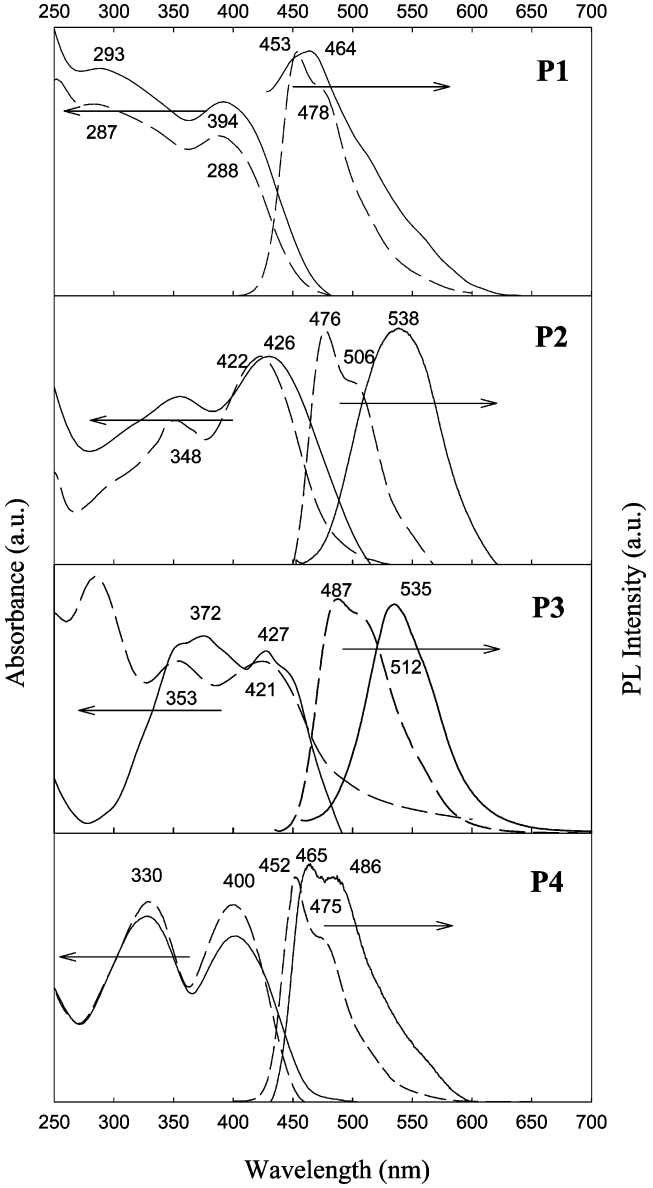

Figure 2. Photoluminescence and UV−vis absorption spectra of **P1**−**P4** in $CHCl_3$ with a concentration of 1×10^{-5} M (- - -) and in films coated on a quartz plate (—). Excitation = 388, 422, 421, and 400 nm for **P1**, **P2**, **P3**, and **P4**, respectively.

conjugation, which is interrupted by ether spacers. Moreover, the PL spectral peaks of **P2** and **P3** shift greatly from 476 and 487 nm in solution to 538 and 535 nm in films coated onto quartz plate, respectively, suggesting the formation of intermolecular excimers[20] in the film state. A similar phenomenon was also observed in **P5** (Scheme 3).[21] However, the red shifts of **P1** and **P4** in the film state are only 11 and 13 nm, respectively, as compared with those in chloroform solution. The results suggest that formation of interchain interaction can probably be reduced by limiting the effective conjugation length. The optical properties of the polymers (**P1**−**P5**) and model compounds (**M1**, **M2**) are summarized in Table 2. As shown in Table 2, the relative PL quantum yields (Φ_{PL}) of **P1** (0.46) and **P2** (0.39) containing triazole segments are lower than those of **P3** (0.54) and **P4** (0.58) possessing oxadiazole segments. Furthermore, the Φ_{PL} of isolated **P4** is higher than fully conjugated **P5** (0.40), and the Φ_{PL} of the twisted **P3** is located between those of **P4** and **P5**. Therefore, confinement of conjugation, whether via

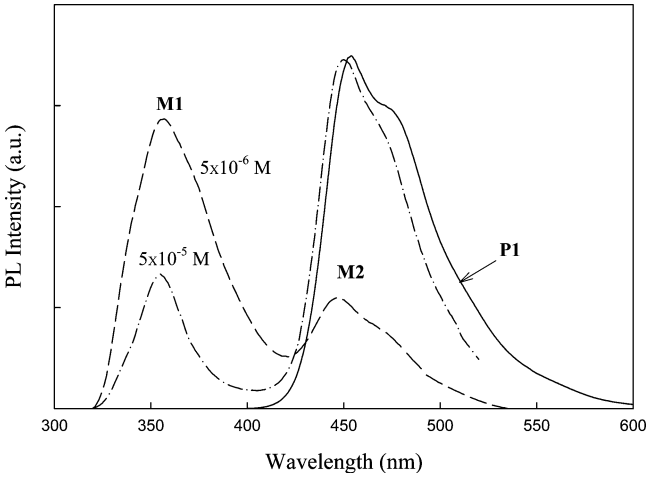

Figure 3. Photoluminescence (excitation = 285 nm) spectra of **P1** (1×10^{-5} M) and a mixture of **M1** and **M2** 5×10^{-6} (—) and 5×10^{-5} M (- · -) in $CHCl_3$.

Table 2. Optical Properties of Model Compounds and Polymers

	UV−vis λ_{max}[a] solution (nm)	UV−vis λ_{max} film (nm)	PL λ_{max}[a] solution (nm)	PL λ_{max} film (nm)	Φ_{PL}[b] solution
P1	287, 388	293, 394	453, 478s	464	0.46
P2	348, 422	426	476, 506s	538	0.39
P3	353, 421	372, 427	487, 512s	535	0.54
P4	330, 400	328, 401	452, 475s	465, 486s	0.58
P5	362s, 442	382s, 459	515, 547s	550	0.40
M1	285		356		
M2	333, 397		449, 466s		

[a] 1×10^{-5} M in $CHCl_3$. s means the wavelength of the shoulder. [b] These values were estimated using quinine sulfate (dissolved in 1 N $H_2SO_{4(aq)}$ with a concentration of 10^{-5} M, assuming Φ_{PL} of 0.55) as a standard. The excitation wavelengths were 350 nm for **P1**−**P5** solutions (10^{-6} M repeating unit at which their absorbance was less than 0.05).

ether spacer or twisted biphenyl linkages, seems to be an effective way to enhance PL quantum yield.

Electrochemical Properties. In our previous studies on copoly(aryl ether)s with isolated alternate hole- and electron-transporting segments we verified that oxidation and reduction start at the former and latter segments, respectively.[6−8] This characteristic is normally found in isolated copolymers and confirms that it can enhance electron and hole affinities simultaneously if proper electron- and hole-transporting segments are incorporated. Isolated **P1** and **P4** are typical copolymers with alternate hole- and electron-transporting segments.

Figure 4a shows the cyclic voltammograms (CVs) of **P1** and **P2** films coated on ITO glass. The onset oxidation and reduction potentials of **P1** are observed at 0.36 and −1.42 V, respectively. It is noteworthy that **P2** shows almost the same potentials (at 0.32 and −1.45 V) as those of **P1**, suggesting that conjugated **P2** and isolated **P1** possess similar electrochemical properties regardless of their structural difference. Accordingly, the biphenyl linkages (between HDB and EDT segments) in **P2** exert a similar effect on the electrochemical property as the ether spacer in **P1**. Bard et al. observed similar results in low molecular weight compounds with a twisted structure between donor and acceptor segments.[12,13]

Optimized molecular geometries for repeat units of **P2**, **P3**, and **P5** (Figure 5) were obtained by minimizing

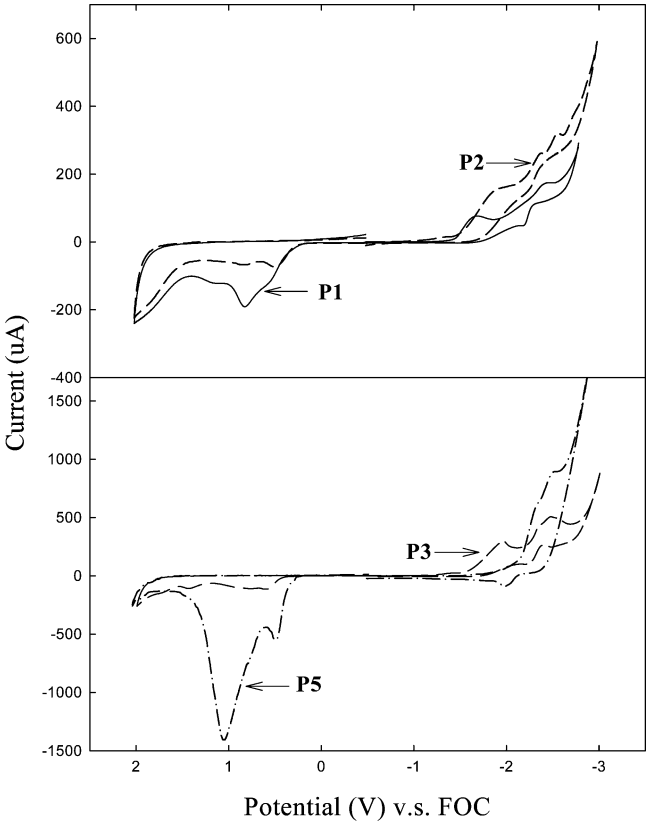

Figure 4. Cyclic voltammograms of **P1** (—), **P2** (– –), **P3** (– –), and **P5** (- · -) (100 mV/s) in film coated on ITO glass electrode in a CH_3CN solution of Bu_4NClO_4 (0.1 M).

energy via semiempirical MNDO calculations in the gas state.[22] Each HDB group in **P2** or **P3** is twisted from the EDO or EDT segment at 83.6° or 89.6°, respectively. However, if the HDB is connected with EDO via a vinylene bond like in **P5**, the torsion is decreased substantially to ca. 1°. Therefore, it is suggested that the twisted structure between hole- (HDB) and electron-transporting segments (EDT or EDO) in **P2** and **P3** effectively limits delocalization of electronic charges as that of the ether spacer does in **P1** and **P4**. Therefore, **P2** and **P3** show similar onset oxidation and reduction potentials to those of **P1** and **P4**, respectively. Furthermore, the oxidation and reduction of **P2** and **P3** would also selectively start at the hole- and electron-transporting segments, respectively. However, as observed in Figure 2, the PL spectral peaks of **P2** and **P3** reveal a red shift of 23 and 35 nm compared to **P1** and **P4**, respectively, suggesting that the torsion in **P2** or **P3** does not completely break conjugation length in polymeric chain.

As shown in Figure 4b the onset oxidation and reduction potentials of **P3** are 0.39 and −1.96 V, respectively, whereas those of **P5** are 0.34 and −2.31 V. This result indicates that **P3** is much more readily reduced than **P5**, but the oxidation tendency is just the opposite. **P3** and **P5** contain the same HDB (hole-transporting) and EDT (electron-transporting) segments, but the linkages between HDB and EDT are the σ-bond and vinylene bond, respectively. Although the conjugated length of **P3** and **P5** is slightly different, clearly the torsion in **P3** also plays an important role in determining its electrochemical property.

Furthermore, in anodic scan **P1**−**P4** exhibit almost the same onset oxidation potentials around 0.36−0.39

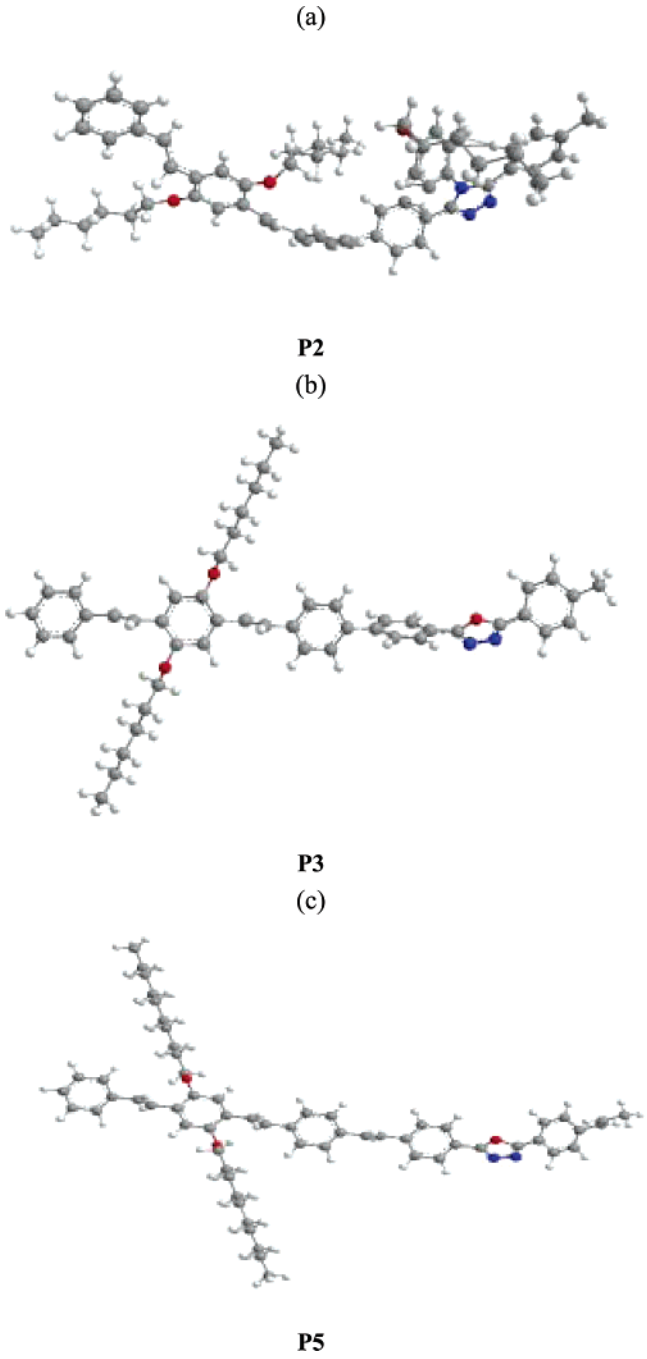

Figure 5. Optimized geometries obtained from semiempirical MNDO calculation for **P2** (a), **P3** (b), and **P5** (c).

V, as shown in Figure 6. This is attributable to the fact that they all contain the same hole-transporting segments (HDBs), regardless of whether the HDBs are linked to electron-transporting segment (EDT or EDO) via ether spacer or σ-bond with torsion. Therefore, it can be concluded that the electron and hole affinities of isolated copoly(aryl ether) (**P1**) or twisted conjugated polymers (**P2** and **P3**) can be engineered similarly by selecting proper hole- and electron-transporting segments.

The highest occupied molecular orbital (HOMO) and lowest unoccupied molecular orbital (LUMO) levels of **P1** can be calculated by comparing with the ferrocence value of −4.8 eV below the vacuum level.[23] For **P2** and **P3**, oxidation and reduction would selectively start at the hole- and electron-transporting segments, respectively. Thus, the HOMO and LUMO energy levels for

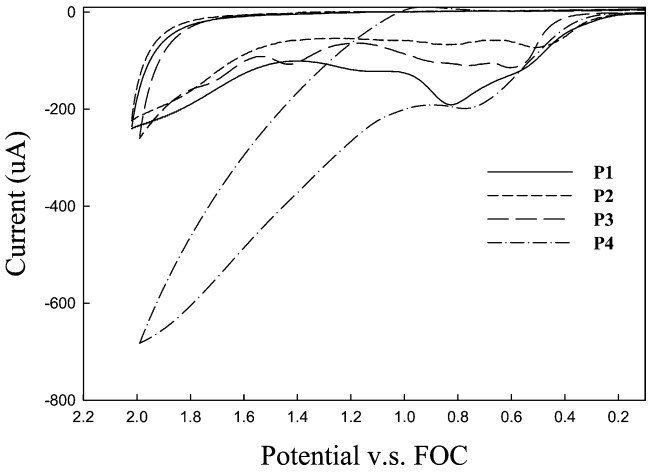

Figure 6. **P1** (—), **P2** (- - -), **P3** (— —), and **P4** (- · -) (100 mV/s) in film coated on ITO glass electrode in a CH_3CN solution of Bu_4NClO_4 (0.1 M).

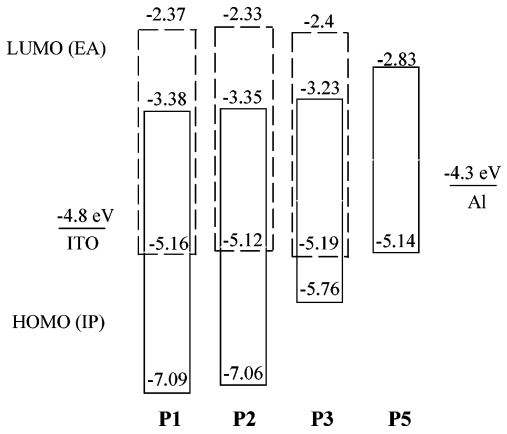

Figure 7. Energy band diagram of **P1**−**P3** (hole-transporting segments, —; electron-transporting segments, - - -) and **P5**.

P2 and **P3** can be estimated similarly as those for **P1**. The HOMO and LUMO energy levels of **P1**, **P2**, and **P3** are −5.16, −5.12, and −5.19 eV and −3.35, −3.38, and −3.23 eV, respectively. The band gaps (E_g^{opt}) for **M1**, **M2**, and **M3**, calculated from their onset of absorption, were 3.71, 2.79, and 2.53 eV. The energy band diagrams of **P1**−**P3** and **P5** are proposed in Figure 7. For **P1**−**P3** the LUMO levels of hole-transporting segments (top horizontal line of the broken rectangle) can be estimated from the HOMO levels of the polymers by adding E_g^{opt} of the corresponding model compounds. The HOMO levels of the electron-transporting segments (bottom horizontal line of the solid rectangle) can be estimated similarly. The electrochemically determined band diagrams of **P1**−**P3** are the overlapped portions of the corresponding composing model compounds. Therefore, hole and electron affinities of **P1**−**P3** can be promoted simultaneously. However, as compared with the LUMO level of conjugated **P5** (−2.83 eV), the twisted **P3** (−3.23 eV) exhibits a lower barrier of electron injection, which is probably attributable to electron-withdrawing aromatic oxadiazole chromophores.

The HOMO energy levels calculated from the semiempirical MNDO method (for instance, −8.50 eV for repeating unit of **P2**) are much lower than those obtained from cyclic voltammograms. However, this large deviation in HOMO energy levels might result from disordered arrangement in polymers, solvation effects, or ion-pair interaction.[13] Therefore, we compare

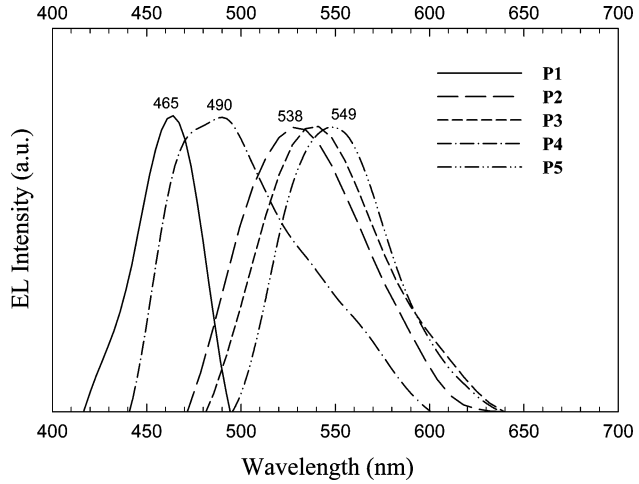

Figure 8. Electroluminescent spectra of **P1**−**P5**.

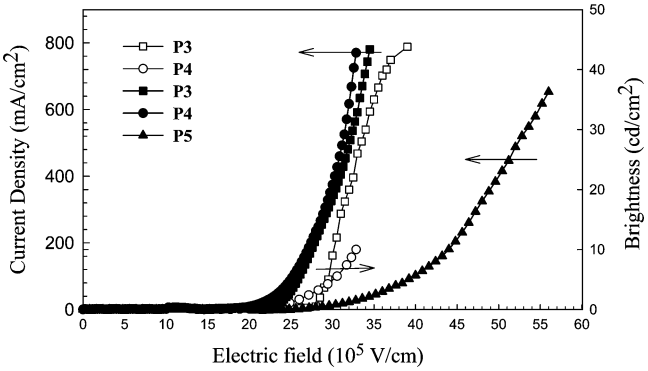

Figure 9. Current density−electric field and brightness−electric field characteristics of the EL devices (ITO/polymer/Al).

energy levels of the repeating unit of **P3** in a coplanar geometry (angle = 0° between each HDB and EDO segments) with those in a twisted geometry (optimized structure of HDB and EDO groups). It is noteworthy that the HOMO and LUMO levels of **P3** in twisted conformation are about 1.24 and 0.72 eV, respectively, higher than those in the coplanar one. This result suggests that the twisted geometry reduces π-electron delocalization and makes it hard to oxidize and reduce.[13]

Device Properties. Figure 8 shows electroluminescence (EL) spectra of single-layer PLED devices (Al/**P1**−**P5**/ITO). The EL spectra are very similar to their PL spectra in films and exhibit blue or yellow electroluminescence. Therefore, similar energy transfer still occurs in isolated copolymers (**P1**, **P4**) during device operation, whereas excimer forms in twisted (**P2**, **P3**) and fully conjugated copolymers (**P5**). The energy transfer of **P1** and **P4** leads to a reduced emission range to improve light purity. It is noteworthy that the current density versus electric field characteristic of **P3** is analogous to that of **P4** and their turn-on electric fields are lower than that of **P5** as shown in Figure 9. This result is coincident with the previous conclusion of comparable electrochemical properties between **P3** (consisting of HDB and EDO via a single bond) and **P4** (consisting of HDB and EDO via ether spacers).

However, in isolated copolymers such as **P4** the hole- and electron-transporting segments might function as hole- and electron-trap centers, respectively, in which conjugation is interrupted by ether spacers. Accordingly, extra energy is required to promote the recombination of electrons and holes in isolated polymers.[18] This drawback is presumably alleviated in **P3** because its conjugation is not broken absolutely. As shown in Figure 9, the maximum brightness of **P3** (43 cd m^{-2}) has improved as compared with **P1** (10 cd m^{-2}). However, its brightness is still lower than **P5** (ca. 1800 cd m^{-2}),[21] which can be attributed to the excimer formation or twisted structure.

Conclusion

Three polymers (**P1**−**P3**) consisting of alternate hole-transporting (HDB) and electron-transporting segments (EDT or EDO) have been synthesized and characterized. Their optical and electrochemical properties have also been studied by comparing with those of polymers **P4** and **P5** containing similar chromophores. From PL spectral investigation it is found that **P1**−**P4** efficiently show energy transfer as compared with a mixture of the corresponding model compounds. Moreover, **P2** and **P3** exhibit interchain interaction (excimer) in the film state. From the cyclic voltammograms the onset oxidation and reduction potentials for **P1** and **P2** are similar. This can be explained by the optimized geometry of **P2** and **P3**, determined from semiempirical MNDO calculations, which shows that HDB and EDT or EDO are twisted 83.6° and 89.6°, respectively. The torsions in **P2** and **P3** significantly limit the delocalization of charge between HDB and EDT or EDO segments. Therefore, the oxidation and reduction would start at the hole- (HDB) and electron-transporting (EDT or EDO) segments, respectively. The HOMO and LUMO energy levels of **P1**, **P2**, and **P3**, estimated from electrochemical data, are −5.16, −5.12, and −5.19 eV and −3.35, −3.38, and −3.23 eV, respectively. The twisted σ-bond in **P2** or **P3** shows a similar effect to the ether spacer in **P1** in interrupting conjugation range. The EL spectra of these copolymers are very similar to their PL spectra in the film state and reveal blue or yellow electroluminescence. The turn-on electric fields of **P3** and **P4** are analogous and lower than that in **P5**, but the brightness of the **P3** device is much higher than that of **P4**.

Acknowledgment. We thank the National Science Council of the Republic of China for financial aid through project NSC 93-2216-E-006-006. We also thank Dr. Shyh-Gang Su, Associate Professor in the Department of Chemistry, National Cheng Kung University of Republic of China, for aid in semiempirical NMDO calculation.

References and Notes

(1) Patra, A.; Pan, H.; Friend, C.-S.; Lin, T.-C.; Cartwright, A.-N.; Prasad, P.-N. *Chem. Mater.* **2002**, *14*, 4044.
(2) Jin, S.-H.; Kim, M.-Y.; Kim, J. Y.; Lee, K.; Gal, Y.-S. *J. Am. Chem. Soc.* **2004**, *126*, 2474.
(3) Liao, L.; Pang, Y.; Ding, L.; Karasz, F. E. *Macromolecules* **2002**, *35*, 3819.
(4) Lee, D. W.; Kwon, K.-Y.; Jin, J.-I.; Park, Y.; Kim, Y.-R.; Hwang, I.-W. *Chem. Mater.* **2001**, *13*, 565.
(5) Jenekhe, S. A.; Lu, L.; Alam, M. M. *Macromolecules* **2001**, *34*, 7315.
(6) Hwang, S.-W.; Chen, Y. *Macromolecules* **2002**, *35*, 5438.
(7) Hwang, S.-W.; Chen, Y.; Chen, S.-H. *J. Polym. Sci., Part B: Polym. Phys.* **2004**, *42*, 333.
(8) Chen, S.-H.; Hwang, S.-W.; Chen, Y. *J. Polym. Sci., Part A: Polym. Chem.* **2004**, *42*, 883.
(9) Sarker, A. M.; Ding, L.; Lahti, P. M.; Karasz, F. F. *Macromolecules* **2002**, *35*, 223.
(10) Liu, B.; Yu, W.-L.; Lai, Y.-H.; Huang, W. *Macromolecules* **2002**, *35*, 4975.

(11) Fan, Q.-L.; Lu, S.; Lai, Y.-H.; Hou, X.-Y.; Huang, H. *Macromolecules* **2003**, *36*, 6976.
(12) Lai, R. Y.; Fabrizio, E. F.; Lu, L.; Jenekhe, S. A.; Bard, A. J. *J. Am. Chem. Soc.* **2001**, *123*, 9112.
(13) Lai, R. Y.; Kong, X.; Jenekhe, S. A.; Bard, A. J. *J. Am. Chem. Soc.* **2003**, *125*, 12631.
(14) Kim, S. W.; Shim, S. C.; Jung, B.-J.; Shim, H.-K. *Polymer* **2002**, *43*, 4297.
(15) Lu, J.; Miyatake, K.; Hlil, A. R.; Hay, A. S. *Macromolecules* **2001**, *34*, 5860.
(16) Shaikh, A. A. G.; Hlil, A. R.; Shaikh, P. A.; Hay, A. S. *Macromolecules* **2002**, *35*, 8728.
(17) Yu, L.-S.; Chen, S.-A. *Adv. Mater.* **2004**, *16*, 774.
(18) Chen, Y.; Hwang, S.-W.; Yu, Y.-H. *Polymer* **2003**, *44*, 3827.
(19) Hwang, S.-W.; Chen, S.-H.; Chen, Y. *J. Polym. Sci., Part A: Polym. Chem.* **2002**, *40*, 2215.
(20) Wu, T.-Y.; Sheu, R.-B.; Chen, Y. *Macromolecules* **2004**, *37*, 725.
(21) Chen, Y.; Sheu, R.-B.; Wu, T. *J. Polym. Sci., Part A: Polym. Chem.* **2003**, *41*, 725.
(22) MNDO semiempirical calculations performed with Gaussian R 98W by Gaussian, Inc.
(23) Liu, Y.; Liu, M. S.; Jen, A. K.-Y. *Acta Polym.* **1999**, *50*, 105.

MA048990M